

Dalton Transactions

Accepted Manuscript



This is an *Accepted Manuscript*, which has been through the Royal Society of Chemistry peer review process and has been accepted for publication.

Accepted Manuscripts are published online shortly after acceptance, before technical editing, formatting and proof reading. Using this free service, authors can make their results available to the community, in citable form, before we publish the edited article. We will replace this *Accepted Manuscript* with the edited and formatted *Advance Article* as soon as it is available.

You can find more information about *Accepted Manuscripts* in the [Information for Authors](#).

Please note that technical editing may introduce minor changes to the text and/or graphics, which may alter content. The journal's standard [Terms & Conditions](#) and the [Ethical guidelines](#) still apply. In no event shall the Royal Society of Chemistry be held responsible for any errors or omissions in this *Accepted Manuscript* or any consequences arising from the use of any information it contains.

Ligand-Coupling Assembly of Re(I) Complexes Containing Pyridyl-Thiolates

Biing-Chiau Tzeng,* An Chao and Manas Banik

Department of Chemistry and Biochemistry, National Chung Cheng University, 168 University Rd.,
Min-Hsiung, Chiayi 62102, Taiwan

Abstract :

By taking advantage of solvothermal reactions of $\text{Re}_2(\text{CO})_{10}$ with 2-mercaptobenzothiazol (HNS_2) or 2-mercaptobenzoxazol (HNOS), a series of Re(I) complexes (**1** - **4**) with *in situ* ligands were synthesized and structurally characterized by X-ray diffraction. In this study, we examined the effects of reaction conditions (i.e., reaction solvents and temperatures) on the HNS_2 system to give complexes **1** - **3**, and also compared the reaction products of the HNS_2 (**2**) and HNOS (**4**) systems in a similar reaction condition. For the HNS_2 system, the reaction temperatures at 140 and 120 °C in mesitylene led to different ligands in complexes **1** and **2**, respectively. However, at the same temperature of 140 °C different solvents (mesitylene or benzene) caused the formation of complexes **1** and **3** containing different ligands, respectively. Although the same temperature and solvent were used, HNS_2 and HNOS underwent a similar *in situ* ligand reaction in dinuclear complexes **2** and **4**, which surprisingly show both *anti* and *syn* conformations, respectively.

Introduction

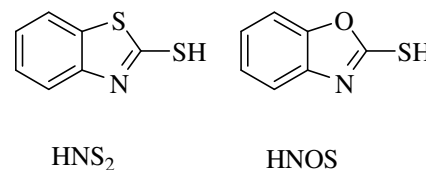
Pyridylthiolates have been known an interesting class of bridging and/or chelating ligands for the construction of various coordination architectures through pyridyl- and/or thiolate-coordination due to their versatile coordinating abilities. Studies focused on metal pyridylthiolates are primarily related to the rich structural diversities,¹ the relevance in biological systems,² and potential applications as precursors for metal-sulfide materials³ and as catalysts for many industrial processes.⁴

Deeming *et al.* used pyridine-2-thiol (pySH) to react with $\text{Re}_2(\text{CO})_{10}$ to give $[\text{Re}_2(\text{CO})_6(\mu\text{-pyS})_2]$ with pyS as a bridging ligand in 1988,⁵ and furthermore $[\text{Re}_2(\text{CO})_6(\mu\text{-pyS})_2]$ and its Mn(I) analogue can find useful applications in the synthesis of tetranuclear heterometallic butterfly clusters of $[\text{M}_2(\text{CO})_6(\mu\text{-pyS})_2]$ (M = Re, Mn) with group VIII metal carbonyls.⁶ It is noted that mixed-metal sulfide clusters in the refluxing toluene solution were afforded due to a C-S bond cleavage reaction. In the meantime, pyridine-2-thiolate (pyS) can be also used as a chelate ligand to form $[\text{Cr}(\text{pyS})_3]$ by reacting with $\text{Cr}(\text{CO})_6$ in the refluxing mesitylene solution.⁷ Surprisingly, a disulfide-bonded adduct of pySS, can be isolated in the $[\text{Cr}(\text{pyS})_2(\text{pySS})]$ complex, where the *in situ* pySS ligand arises from the coupling of pyridine-2-thiol with sulfur. In fact, a similar disulfide-bonded adduct has been also found in the 2-mercapto-1-methylimidazolate ($\text{SN}_2\text{C}_4\text{H}_5$) system.⁸

Solvothermal *in situ* metal/ligand reactions in the presence of metal ions can provide a good chance for the generation of new ligands, leading to the synthesis of functional coordination frameworks and new materials.⁹ Thus, it really owns the potential to be developed as a new strategy for the *in situ* synthesis of new ligands and construction of interesting polymeric frameworks. In this regard, Feng *et al.* took advantage of solvothermal *in situ* ligand synthesis through disulfide cleavage from 4,4'-dithiodipyridine to give pyridine-4-thiolate (4-pyt) acting as bridging ligands for the formation of interesting 2- and 3-D coordination polymers.¹⁰ Tong *et al.* also reported three new copper(I) cluster-based coordination networks, $[\text{Cu}_4\text{I}_4(\text{tdp})_2]$, $[\text{Cu}_5\text{I}_5(\text{ptp})_2]$, and $[\text{Cu}_6\text{I}_6(\text{ptp})_2]$ (tdp = 4,4'-thiodipyridine and ptp = 1-(4-pyridyl)-4-thiopyridine),¹¹ where the tdp and ptp ligands were generated from the *in situ* cleavage and rearrangement reactions of the 4,4'-dithiodipyridine (4-dtdp) ligand in the presence of Cu(I) ions. In fact, the *in situ* ligand formation, such as the formation of tdp or ptp mentioned above through both the S-S bond cleavage and the S-C(sp²) bond cleavage and

rearrangement reactions, was tentatively ascribed to the free-radical mechanism.

As a part of our continuing interest in metal pyridylthiolate complexes,¹² we report herein a series of Re(I) complexes containing the *in situ* ligands from the reactions of $\text{Re}_2(\text{CO})_{10}$ with two structural analogues of HNS_2 and HNOS under solvothermal conditions.



Experimental Section

General Information and Physical Measurements. 2-Mercaptobenzothiazol (HNS_2) and 2-mercaptobenzoxazol (HNOS) were purchased from Aldrich Chemicals. $\text{Re}_2(\text{CO})_{10}$ was purchased from Strem Chemicals. All solvents (Analytical grade) for synthesis were used without further purification. Since the crystal structure of $[\text{Re}_2(\mu\text{-NS}_2)_2(\text{CO})_6]$ (**1**) has been determined very recently,¹³ we have only described the alternative solvothermal synthesis. Infrared (IR) spectra were recorded with samples in the form of KBr pellets on a Perkin-Elmer PC 16 FTIR spectrometer. Solid-state emission spectra at room temperature and at 77 K were recorded on a Hitachi F-7000 spectrophotometer. The powder X-ray diffraction (PXRD) data were recorded on a Shimadzu XRD-6000 diffractometer. Elemental analysis (EA) of the complexes was performed on an Elementar vario EL III Heraeus CHNOS Rapid F002 elemental analyzer and the solid samples were pre-treated by subjecting to a vacuum overnight.

Solvothermal Synthesis. $[\text{Re}_2(\mu\text{-NS}_2)_2(\text{CO})_6]$ (**1**). $\text{Re}_2(\text{CO})_{10}$ (0.020 g, 0.03 mmol) and HNS_2 (0.020 g, 0.12 mmol) were stirred in a mesitylene solution (2.0 mL) for 10 min in air. The mixture was transferred to a 25 mL Teflon reactor, sealed, and heated in an oven to 140 °C for 48 h. After gradual cooling to room temperature the filtrate was stood in air for three days, deep brown crystals were obtained and then filtered, washed, and dried in the air (0.015 g, yield *ca.* 58 %). Anal. Calcd (%) for $\text{C}_{20}\text{H}_8\text{N}_2\text{O}_6\text{Re}_2\text{S}_4$: C 27.50, H 0.90, N 3.20, S 14.50; found: C 27.82, H 0.65, N 3.27, S 14.45. FT-IR : $\nu_{\text{CO}} = 2037, 2021, 1959, \text{ and } 1915 \text{ cm}^{-1}$; $\nu_{\text{C=N}} = 1634 \text{ cm}^{-1}$; $\nu_{\text{C=C}} = 1561 \text{ and } 1459 \text{ cm}^{-1}$.

$[\text{Re}_2(\mu\text{-NS}_2\text{S})_2(\text{CO})_6]$ (**2**). $\text{Re}_2(\text{CO})_{10}$ (0.020 g, 0.03 mmol) and HNS_2 (0.020 g, 0.12 mmol) were

stirred in a mesitylene solution (2.0 mL) for 10 min in air. The mixture was transferred to a 25 mL Teflon reactor, sealed, and heated in an oven to 120 °C for 48 h. After gradual cooling to room temperature yellow crystals were obtained and then filtered, washed, and dried in the air (0.014 g, yield *ca.* 45 %). Anal. Calcd (%) for C₂₀H₈N₂O₆Re₂S₆ : C 25.63, H 0.86, N 2.99, S 20.53; found: C 26.05, H 0.98, N 2.88, S 20.63. FT-IR : $\nu_{\text{CO}} = 2014, 1943, \text{ and } 1901 \text{ cm}^{-1}$; $\nu_{\text{C=N}} = 1636 \text{ cm}^{-1}$; $\nu_{\text{C=C}} = 1566 \text{ and } 1447 \text{ cm}^{-1}$.

[Re(CO)₃(NS₂NS)(SH)] (3). Re₂(CO)₁₀ (0.020 g, 0.03 mmol) and HNS₂ (0.020 g, 0.12 mmol) were stirred in a benzene solution (2.0 mL) for 10 min in air. The mixture was transferred to a 25 mL Teflon reactor, sealed, and heated in an oven to 140 °C for 48 h. After gradual cooling to room temperature the filtrate was stood in air for three days, deep brown crystals were obtained and then filtered, washed, and dried in the air (0.006 g, yield *ca.* 36 %). Anal. Calcd (%) for C₁₇H₉N₂O₃ReS₄ : C 33.82, H 1.50, N 4.64, S 21.24; found: C 33.81, H 1.36, N 4.34, S 21.34. FT-IR : $\nu_{\text{CO}} = 2018, 1910, \text{ and } 1885 \text{ cm}^{-1}$; $\nu_{\text{C=N}} = 1637 \text{ cm}^{-1}$; $\nu_{\text{C=C}} = 1561 \text{ and } 1451 \text{ cm}^{-1}$.

[Re₂(μ -NOSS)₂(CO)₆] (4). Re₂(CO)₁₀ (0.020 g, 0.03 mmol) and HNOS (0.018 g, 0.12 mmol) were stirred in a mesitylene or benzene solution (2.0 mL) for 10 min in air. The mixture was transferred to a 25 mL Teflon reactor, sealed, and heated in an oven to 120 or 140 °C for 48 h. After gradual cooling to room temperature yellow crystals were obtained and then filtered, washed, and dried in the air (0.015 g, yield *ca.* 55 %). Anal. Calcd (%) for C₂₀H₈N₂O₈Re₂S₄ : C 26.50, H 0.90, N 3.10, S 14.10; found: C 26.75, H 0.75, N 3.32, S 14.15. FT-IR : $\nu_{\text{CO}} = 2034, 1943, \text{ and } 1906 \text{ cm}^{-1}$; $\nu_{\text{C=N}} = 1637 \text{ cm}^{-1}$; $\nu_{\text{C=C}} = 1440 \text{ cm}^{-1}$.

X-ray Crystallography

Suitable crystals were mounted on glass capillaries. Data collection was carried out on a Bruker SMART CCD diffractometer with Mo radiation (0.71073 Å) at 150(2), 295(2), and 293(2) K for complexes **2** - **4**, respectively. A preliminary orientation matrix and unit cell parameters were determined from 3 runs of 15 frames each, each frame corresponding to 0.3° scan in 20 s, followed by spot integration and least-square refinement. Data were measured using an ω scan of 0.3° per frame for 20 s until a complete hemisphere had been collected. Cell parameters were retrieved using

SMART^{14a} software and refined with SAINT^{14b} on all observed reflections. Data reduction was performed with the SAINT software and corrected for Lorentz and Polarization effects. Absorption corrections were applied with the program SADABS.^{14c} The structure was solved by direct methods with the SHELXS-97^{14d} program and refined by full-matrix least-squares methods on F^2 with SHELXL-97.^{14e} All non-hydrogen atomic positions were located in difference Fourier maps and refined anisotropically. Hydrogen atoms were constrained to the ideal geometry using an appropriate riding model. Detailed data collection and refinement of complexes **2** - **4** are summarized in Table 1 and their selected bond distances and angles are also tabulated in Table 2.

Results and Discussion

In this study, we investigated the solvothermal reactions of $\text{Re}_2(\text{CO})_{10}$ with HNS_2 or HNOS , two structurally similar bridging ligands. Firstly, we examined the effects of reaction conditions (i.e., reaction solvents and temperatures) on the HNS_2 system, and fortunately three different complexes of **1** - **3** without or with *in situ* ligands can be obtained depending on the reaction conditions used. Secondly, the HNS_2 and HNOS systems were also compared with the reaction products in a similar reaction condition. In spite of similar *in situ* ligands formed in complexes **2** and **4**, two different conformations (*anti* and *syn* forms) were serendipitously isolated. The ligand coupling reactions in this study are summarized in Scheme 1.

Description of Crystal Structures

The molecular structure of **2** is shown in Figure 1, which crystallized in the space group of $P\bar{1}$. The molecule, with a center of inversion, consists of a dinuclear structure of two $\text{Re}(\text{I})$ ions with six terminal carbonyl groups and two $\mu\text{-NS}_2\text{S}$ ligands. A remarkable structural feature of **2** is the *in situ* ligand formation of the $\mu\text{-NS}_2\text{S}$ ligand with a bridging sulfide atom resulting from the C-S bond cleavage of another NS_2 ligand. Each $\mu\text{-NS}_2\text{S}$ ligand bridges two $\text{Re}(\text{I})$ ions through the sulfur atom while the nitrogen atom coordinates to one $\text{Re}(\text{I})$ ion to form a five-membered chelate ring. Each octahedral $\text{Re}(\text{I})$ ion is also bonded with three carbonyl groups in a facial arrangement. The structure of **2** is indeed similar to that of $[\text{Fe}_2(\text{CO})_6(\mu\text{-S}_2\text{N}_2\text{C}_4\text{H}_5)_2]$,⁸ and both complexes also contain two *in situ* ligands on the different sides of the M_2S_2 ring as an *anti* form of complexes. The Re-N and Re-S bond

distances in **2** (Re(1)-N(1) 2.232(3) Å; Re(1)-S(3) 2.4795(12), Re(1)-S(3A) 2.5194(12) Å) are comparable to those in **1**¹³ and the Re...Re distance is also pretty long (3.816(1) Å) and indicative of a nonbonding distance. The S(2)-S(3) distance of 2.0767(14) Å is similar to the related value of 2.0810(10) Å in [Fe₂(CO)₆(μ-S₂N₂C₄H₅)₂].⁸

As shown in Figure 2, the molecular structure of **3** shows a mononuclear complex, which crystallized in the space group of P2₁/c. The molecule consists of a mononuclear Re(I) ion with three terminal carbonyl groups, one chelating NS₂NS, as well as one SH⁻ ligand. Remarkably, the structural feature of **3** is the *in situ* ligand formation of the μ-NS₂S ligand, originating from a C-S cross-coupling reaction of NS₂ ligands. However, such an *in situ* reaction has been observed for the reaction between HNS₂ and CuI leading to [CuI(NS₂NS)]₂.¹⁵ Each NS₂NS ligand coordinates to the Re(I) ion through two nitrogen atoms to form a six-membered chelate ring and each octahedral Re(I) ion is also bonded with three carbonyl groups in a facial arrangement and a hydrogen sulfide (SH⁻),¹⁶ a byproduct of the coupling reaction. Unlike that of [CuI(NS₂NS)]₂, complex **3** simultaneously isolated two coupling products (NS₂NS and SH⁻) as coordinating ligands in a single complex. The hydrosulfido complexes have been known in the literature.¹⁶ The Re-N and Re-S bond distances in **3** (Re(1)-N(1) 2.207(4), Re(1)-N(2) 2.213(4) Å; Re(1)-S(4) 2.4719(14) Å) are comparable to those in **1**, **2**, and [Re(SH)(CO)₃(bpy)]₂ (bpy = 2,2'-bipyridine; Re(1)-S(1) 2.514(2) Å).^{16b}

The molecular structure of **4** is displayed in Figure 3, which crystallized in the space group of C2/c. The molecule, with two-fold axis passing through its center, consists of a dinuclear structure of two Re(I) ions with six terminal carbonyl groups and two μ-NOSS ligands, which are an analogue of the *in situ* μ-NS₂S ligand. Each μ-NOSS ligand bridges two Re(I) ions through the sulfur atom while the nitrogen atom coordinates to one Re(I) ion to form a five-membered chelate ring. Each octahedral Re(I) ion is also bonded with three carbonyl groups in a facial arrangement. Surprisingly, unlike that of **2** the structure of **4** contains two *in situ* μ-NOSS ligands on the same side of the Re₂S₂ ring. The Re₂S₂ ring is nearly planar (a dihedral angle of 178.1° between Re(1)-S(2)-Re(1A) and Re(1)-S(2A)-Re(1A) planes), which is similar to the Re₂S₂ ring in **2** and the Fe₂S₂ core in [Fe₂(CO)₆(μ-S₂N₂C₄H₅)₂].⁸ In addition, the molecule adopts a chiral structure with C₂ symmetry and the overall achiral structure is exactly analogous to [Mn₂(CO)₆(μ-pyS)₂],¹¹ [Re₂(CO)₆(μ-MepyS)₂],⁵ and [Mn₂(CO)₆(μ-SN₂C₄H₅)₂].¹² The Re-N and Re-S bond distances in **4** (Re(1)-N(1) 2.193(3) Å; Re(1)-

S(2) 2.4925(8), Re(1)-S(2A) 2.5135(8) Å) are also comparable to those in **1** - **3** and the Re...Re distance is long (3.806 Å) and indicative of a nonbonding distance as well. The S(1)-S(2) distance of 2.0867(9) Å is also similar to the related values of 2.0767(14) Å in **2** and 2.0810(10) Å in [Fe₂(CO)₆(μ-S₂N₂C₄H₅)₂].⁸

From solvothermal reactions of HNS₂ with Re₂(CO)₁₀, it is remarkable that temperature and solvent effects leading to the formation of three different complexes (**1** - **3**) based on NS₂ and two *in situ* NS₂S and NS₂NS ligands can be observed. In addition, complexes **2** and **4** are synthesized in a similar reaction condition, and they do contain structurally similar *in situ* ligands of NS₂S and NS₂NS, respectively. However, *anti* and *syn* conformations for dinuclear structures of **2** and **4** have been isolated, respectively. Significantly, even though the reaction conditions for the HNOS system are tuned (i.e., from mesitylene to benzene, from 120 to 140 °C, or metal to ligand ratios from 1:1, 1:2, or 1:4), complex **4** can be isolated as the only product. Although the HNS₂ or HNOS ligands represent two structural analogues of bridging ligands, the small difference between atoms' size and electronegativity of S and O atoms may be large enough to lead to a delicate effect on the assembly process. Unfortunately, we cannot well explain such a distinction point observed for the HNS₂ or HNOS systems at this moment.

To ascertain the purities of complexes **1** - **4**, we carried out powder X-ray diffraction (PXRD) studies. The PXRD patterns of **1** - **4** (see the supporting information) all match well with those of the respective simulated ones obtained from single crystal data, suggesting that their pure phases in the solid state have been obtained in this study.

Solid-State Emission Spectra

Complexes **1** - **4** are all emissive for solid samples, and hence the emission spectra of **1** - **4** are measured at room temperature and at 77 K (see supporting information). Upon photoexcitation at 240 nm, solid samples of **1** - **3** at room temperature and at 77 K show emissions with maxima at *ca.* 390 and 384 nm, respectively. These emissions are similar to *ca.* 396 and 389 nm at room temperature and at 77 K for the HNS₂ ligand respectively, and hence they have been assigned to an intraligand transition of HNS₂. For complex **4**, solid samples also show emission maxima at *ca.* 380 and 385 nm

at room temperature and at 77 K respectively, which are also similar to *ca.* 391 and 385 nm at room temperature and at 77 K for the HNOS ligand respectively, and hence they have been assigned to an intraligand transition of HNOS as well. Unfortunately, no metal and/or ligand effect on such emissions for complexes **1** - **4** can be observed.

Conclusions

In this study, a series of Re(I) complexes (**1** - **4**) with *in situ* ligands, assembled from solvothermal reactions of $\text{Re}_2(\text{CO})_{10}$ with HNS_2 or HNOS, were synthesized and structurally characterized by X-ray diffraction. It is noted that three *in situ* ligands involved in coordination chemistry with Re(I) ions have been found depending on the respective reaction conditions (i.e., reaction solvents and temperatures) and different ligands used in the reactions. For the HNS_2 system, the reaction temperatures at 140 and 120 °C in mesitylene led to different ligands in complexes **1** and **2**, respectively. However, at the same temperature of 140 °C different solvents (mesitylene or benzene) caused the formation of complexes **1** and **3** containing different ligands, respectively. Although the same temperature and solvent were used, HNS_2 or HNOS underwent a similar *in situ* ligand reaction in dinuclear complexes **2** and **4**, which surprisingly show both *anti* and *syn* conformations, respectively. The above results suggest that the current synthetic scheme taking advantage of solvothermal reactions possibly provides a useful approach to construct various coordination architectures.

Acknowledgement

We thank the National Science Council and National Chung Cheng University of Taiwan for financial support.

References :

1. (a) S. G. Rosenfield, S. A. Swedberg, S. K. Arora and P. K. Mascharak, *Inorg. Chem.*, 1986, **25**, 2109; (b) A. J. Deeming, K. I. Hardcastle, M. N. Meah, P. A. Bates, H. M. Dawes and M. B. Hursthouse, *J. Chem. Soc., Dalton Trans.*, 1988, 227; (c) A. J. Deeming, M. Karim and M. Powell, *J. Chem. Soc., Dalton Trans.*, 1990, 2321; (d) D. J. Rose, Y.-D. Chang, Q. Chen and J. Zubieta, *Inorg. Chem.*, 1994, **33**, 5167; (e) S. Kitagawa, M. Munakata, H. Shimono, S. Matsuyama and S. Masuda, *J. Chem. Soc., Dalton Trans.*, 1990, 2105; (f) K. Umakoshi, A. Ichimura, I. Kinoshita and S. Ooi, *Inorg. Chem.*, 1990, **29**, 4005; (g) P. Mura, B. J. Olby and S. D. Robinson, *J. Chem. Soc., Dalton Trans.*, 1985, 2101; (h) B. K. Santra, M. Menon, C. K. Pal and G. K. Lahiri, *J. Chem. Soc., Dalton Trans.*, 1997, 1387; (i) S. E. Kabir, M. M. Karim, K. Kundu, S. M. Bashir Ullah and K. I. Hardcastle, *J. Organomet. Chem.*, 1996, **517**, 155.
2. (a) S. G. Rosenfield, H. P. Berends, L. Gelmini, D. W. Stephan and P. K. Mascharak, *Inorg. Chem.*, 1987, **26**, 2792; (b) R. Castro, M. L. Durán, J. A. García-Vázquez, J. Romero, A. Sousa, A. Castiñeiras, W. Hiller and J. Strähle, *J. Chem. Soc., Dalton Trans.*, 1990, 531; (c) C. O. Kienitz, C. Thöne and P. G. Jones, *Inorg. Chem.*, 1996, **35**, 3990.
3. (a) M. Berardini and J. Brennan, *Inorg. Chem.*, 1995, **34**, 6179; (b) D. J. Rose, Y.-D. Chang, Q. Chen, P. B. Kettler and J. Zubieta, *Inorg. Chem.*, 1995, **34**, 3973; (c) Y. Cheng, T. J. Emge and J. G. Brennan, *Inorg. Chem.*, 1996, **35**, 342; (d) J. Lee, T. J. Emge and J. G. Brennan, *Inorg. Chem.*, 1997, **36**, 5064.
4. E.I. Stiefel, K. Matsumoto (Eds.), *Transition Metal Sulfur Chemistry: Biological and Industrial Significance*, ACS Symposium series 653, American Chemical Society, Washington DC, 1996.
5. A. J. Deeming, M. Karim, P. A. Bates and M. B. Hursthouse, *Polyhedron*, 1988, **7**, 1401.
6. (a) A. J. Deeming, M. Karim, N. I. Powell and K. I. Hardcastle, *Polyhedron*, 1990, **9**, 623; (b) B. Cockerton, A. J. Deeming, M. Karim and K. I. Hardcastle, *J. Chem. Soc., Dalton Trans.*, 1991, 431; (c) S. Ghosh, K. N. Khanam, G. M. Golzar Hossain, D. T. Haworth, S. V. Lindeman, G. Hogarth and S. E. Kabir, *New J. Chem.*, 2010, **34**, 1875.
7. A. Sousa-Pedrares, M. L. Durán-Carril, J. Romero, J. A. García-Vázquez and A. Sousa, *Polyhedron*, 2013, **62**, 278.
8. S. Ghosh, S. E. Kabir, S. Pervin, G. M. Golzar Hossain, D. T. Haworth, S. V. Lindeman, T. A. Siddiquee, D. W. Bennett and H. W. Roesky, *Z. Anorg. Allg. Chem.* 2009, **635**, 76.
9. (a) Constable, E. C. *Metals and Ligand Reactivity (New, revised and expanded edition)*; VCHM: Weinheim, Germany, 2005; (b) J. Burgess and C. D. Hubbard, *Adv. Inorg. Chem.*, 2003, **54**, 71; (c) X.-M. Zhang, *Coord. Chem. Rev.*, 2005, **249**, 1201; (d) X.-M. Chen and M.-L. Tong, *Acc. Chem. Res.*, 2007, **40**, 162.
10. L. Han, X. H. Bu, Q. C. Zhang and P. Y. Feng, *Inorg. Chem.*, 2006, **45**, 5736.

11. (a) J. Wang, S.-L. Zheng, S. Hu, Y.-H. Zhang and M.-L. Tong, *Inorg. Chem.*, 2007, **46**, 795; (b) J. Wang, Y.-H. Zhang, H.-X. Li, Z.-J. Lin and M.-L. Tong, *Cryst. Growth Des.*, 2007, **11**, 2352.
12. (a) B.-C. Tzeng, C.-S. Ding, T.-Y. Chang, C.-C. Hu and G.-H. Lee, *CrystEngComm*, 2012, **14**, 8228; (b) B.-C. Tzeng, T.-H. Chiu, S.-Y. Lin, C.-M. Yang, T.-Y. Chang, C.-H. Huang, A. H.-H. Chang and G.-H. Lee, *Cryst. Growth Des.*, 2009, **9**, 5356; (c) B.-C. Tzeng, Y.-L. Wu, G.-H. Lee and S.-M. Peng, *New J. Chem.*, 2007, **31**, 199; (d) B.-C. Tzeng, W.-H. Liu, J.-H. Liao, G.-H. Lee and S.-M. Peng, *Cryst. Growth Des.*, 2004, **4**, 573; (e) B.-C. Tzeng, Y.-C. Huang, W.-M. Wu, S.-Y. Lee, G.-H. Lee and S.-M. Peng, *Cryst. Growth Des.*, 2004, **4**, 63; (f) B.-C. Tzeng, G.-H. Lee, S.-M. Peng, *Inorg. Chem. Commun.*, 2004, **7**, 151.
13. S. Ghosh, K. N. Khanam, M. K. Hossain, G. M. Golzar Hossain, D. T. Haworth, S. V. Lindeman, G. Hogarth and S. E. Kabir, *J. Organomet. Chem.*, 2010, **695**, 1146.
14. (a) SMART V5.625 Software for the CCD Detector System, Bruker-AXS Instruments Division, Madison, WI, 2000; (b) SAINT V6.22 Software for the CCD Detector System, Bruker-AXS Instruments Division, Madison, WI, 2000; (c) G.M. Sheldrick, SADABS, V 2.03, University of Göttingen, Germany, 2002; (d) Sheldrick, G. M. SHELXL-97, *Acta Crystallogr.*, 2008, **A64**, 112; (e) G. M. Sheldrick, SHELXL-97, University of Göttingen, Germany, 1997.
15. W.-X. Zhou, B. Yin, J. Li, W.-J. Sun, F.-X. Zhang, *Inorg. Chim. Acta*, 2013, **408**, 209.
16. (a) F. Bock, F. Fischer, K. Radacki and W. A. Schenk, *Eur. J. Inorg. Chem.*, 2010, **391**; (b) D. C. Gerbino, E. Hevia, D. Morales, M. E. Navarro Clemente, J. Pérez, L. Riera, V. Riera and D. Miguel, *Chem. Commun.*, 2003, 328; (c) D. E. Schwarz, J. A. Dopke, T. B. Rauchfuss and S. R. Wilson, *Angew. Chem., Int. Ed.*, 2001, **40**, 2351.

Scheme 1 Ligand Coupling Reactions.

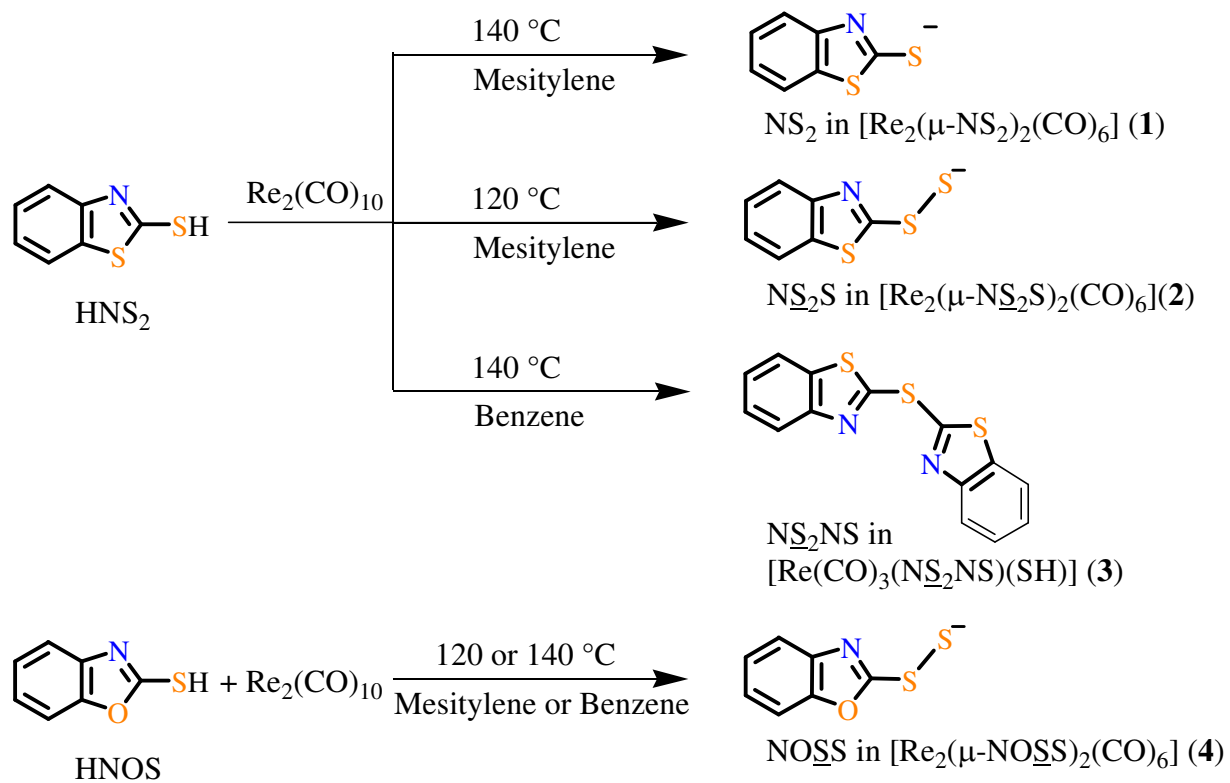


Table 1 Crystallographic Data of **2 - 4**.

	2	3	4
Empirical formula	C ₂₀ H ₈ N ₂ O ₆ Re ₂ S ₆	C ₁₇ H ₉ N ₂ O ₃ ReS ₄	C ₂₀ H ₈ N ₂ O ₈ Re ₂ S ₄
Formula weight	937.04	603.70	904.98
Crystal system	Triclinic	Monoclinic	Monoclinic
Space group (No.)	P $\bar{1}$	P2 ₁ /c	C2/c
a (Å)	7.431(3)	15.037(4)	21.293(3)
b (Å)	9.156(4)	8.393(2)	12.0998(18)
c (Å)	9.918(4)	14.851(4)	9.2966(14)
α (°)	73.722(6)		
β (°)	70.374(6)	95.905(5)	107.951(5)
γ (°)	74.707(6)		
V (Å ³), Z	599.3(5), 1	1864.3(9), 4	2278.6(6), 4
F(000) (e)	436	1152	1679
μ (Mo-K α) (mm ⁻¹)	10.656	6.987	11.035
T (K)	150(2)	295(2)	293(2)
Reflections collected	6965	21171	12800
Independent reflections (Fo \geq 2 σ (Fo))	2804 (R _{int} =0.0385)	4515 (R _{int} =0.0407)	2753 (R _{int} =0.0365)
Refined parameters	179	277	179
Goodness-of-fit on F ²	1.080	1.048	1.221
R ^a , R _w ^b (I \geq 2 σ (I))	0.0191, 0.0461	0.0325, 0.0659	0.0167, 0.0448
R ^a , R _w ^b (all data)	0.0198, 0.0466	0.0476, 0.0733	0.0172, 0.0451

$${}^a R = \frac{\sum ||F_o| - |F_c||}{\sum |F_o|}, \quad {}^b wR_2 = \left\{ \frac{\sum w(F_o^2 - F_c^2)^2}{\sum [w(F_o^2)^2]} \right\}^{1/2}.$$

Table 2 Selected Bond Distances (Å) and Angles (°) of **2** - **4**.

Compound				
2^a	Re(1)–C(2)	1.919(4)	Re(1)–C(3)	1.919(3)
	Re(1)–C(1)	1.927(4)	Re(1)–N(1)	2.232(3)
	Re(1)–S(3)	2.4795(12)	Re(1)–S(3A)	2.5194(12)
	S(2)–S(3)	2.0767(14)		
	N(1)–Re(1)–S(3)	82.26(7)	N(1)–Re(1)–S(3A)	83.65(7)
	S(3)–Re(1)–S(3A)	80.49(3)		
3	Re(1)–C(3)	1.905(6)	Re(1)–C(2)	1.907(6)
	Re(1)–C(1)	1.910(5)	Re(1)–N(1)	2.207(4)
	Re(1)–N(2)	2.213(4)	Re(1)–S(4)	2.4719(14)
	N(1)–Re(1)–N(2)	84.17(15)	N(1)–Re(1)–S(4)	85.26(11)
	N(2)–Re(1)–S(4)	83.43(11)		
4^b	Re(1)–C(1)	1.928(3)	Re(1)–C(3)	1.930(3)
	Re(1)–C(2)	1.932(4)	Re(1)–N(1)	2.193(3)
	Re(1)–S(2)	2.4925(8)	Re(1)–S(2A)	2.5135(8)
	S(1)–S(2)	2.0867(9)		
	N(1)–Re(1)–S(2)	82.76(6)	N(1)–Re(1)–S(2A)	91.20(6)
	S(2)–Re(1)–S(2A)	81.02(3)		

^a -x+2, -y+1, -z; ^b -x+2, y, -z+3/2

Caption of Figures

Figure 1. A crystal structure of **2** with the ORTEP diagram showing 50 % probability ellipsoids.

Figure 2. A crystal structure of **3** with the ORTEP diagram showing 50 % probability ellipsoids.

Figure 3. A crystal structure of **4** with the ORTEP diagram showing 50 % probability ellipsoids.

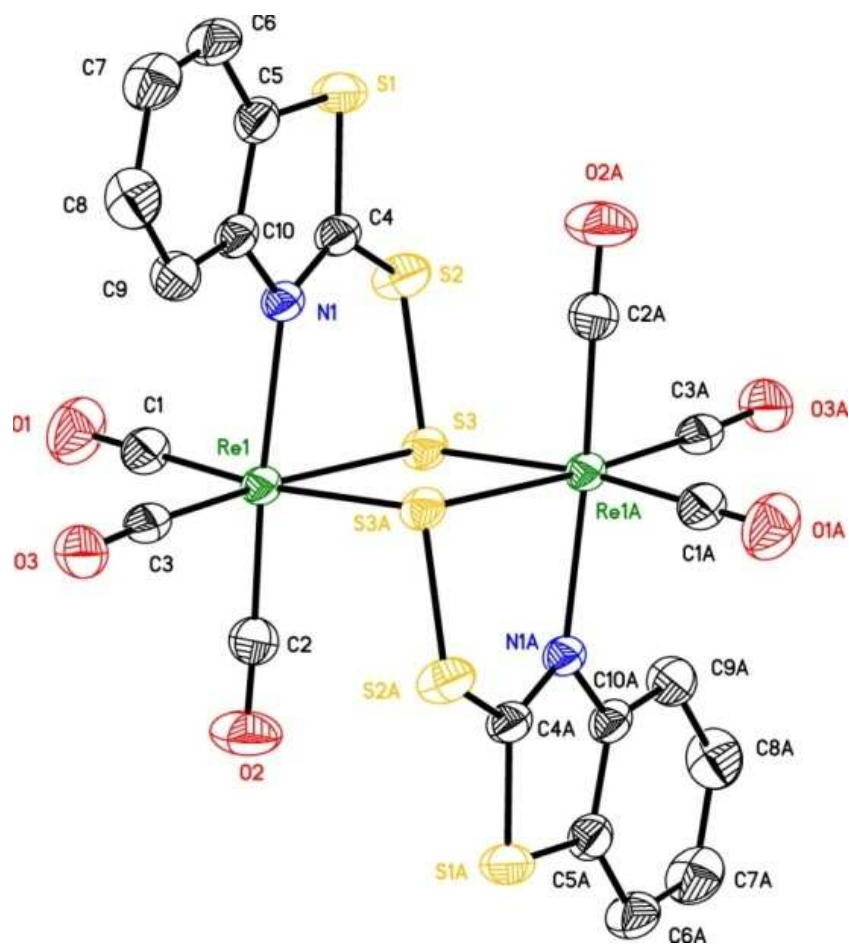


Figure 1

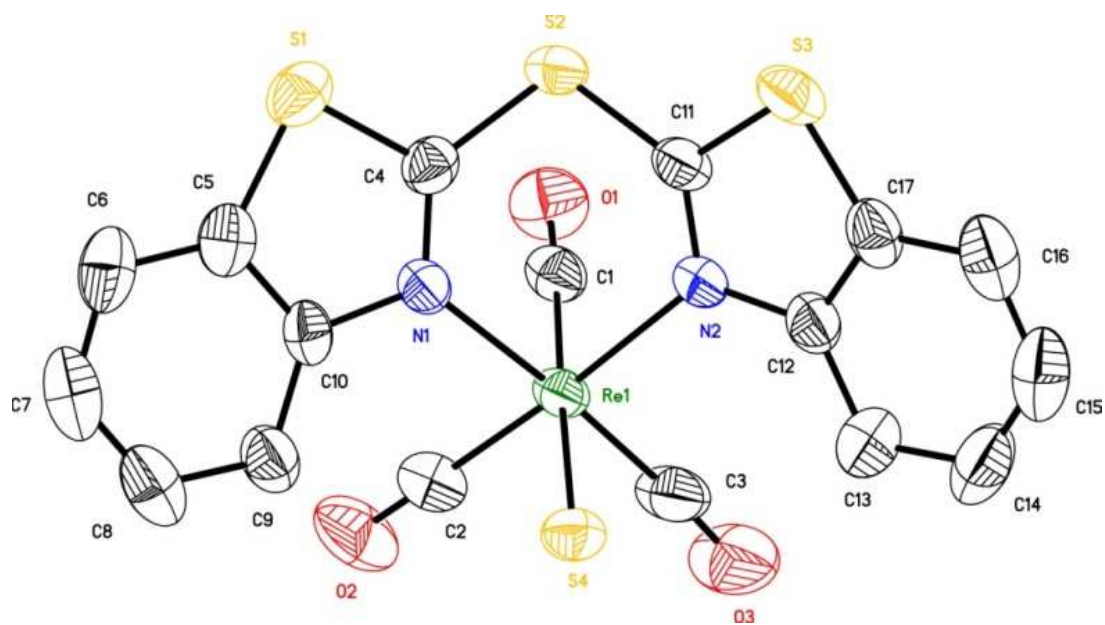


Figure 2

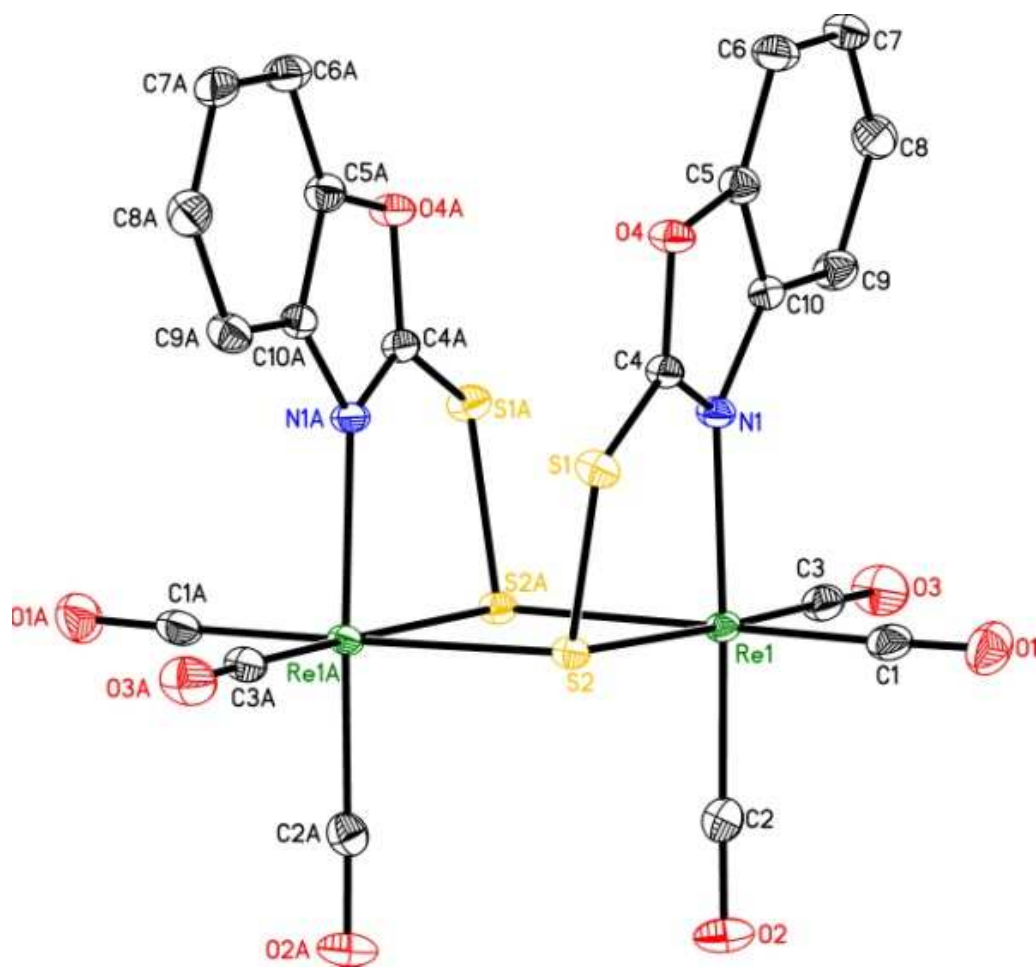
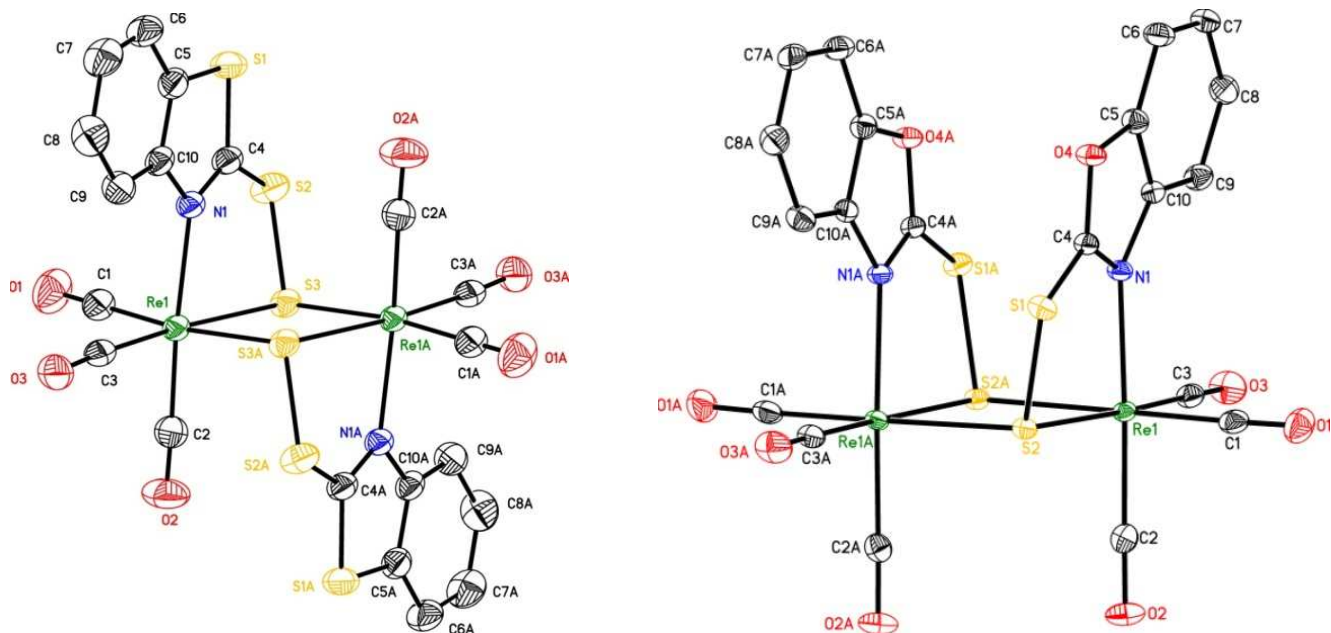


Figure 3

Graphic abstract



Complexes **2** and **4** were synthesized in a similar reaction condition, except that different ligands of HNS₂ and HNOS were used respectively. Two dinuclear structures of **2** and **4** with two similar *in situ* ligand analogues show distinct conformations, *anti* and *syn* forms, respectively.